Chemical Engineering Journal 162 (2010) 1035–1044

Contents lists available at ScienceDirect

Chemical Engineering Journal

journal homepage: www.elsevier.com/locate/cej

Polymeric Fe/Zr pillared montmorillonite for the removal of Cr(VI) from aqueous solutions

Jianbing Zhou[a,b], Pingxiao Wu[a,b,c,*], Zhi Dang[a,b,c], Nengwu Zhu[a,b,c], Ping Li[a,b], Jinhua Wu[a,b], Xiangde Wang[a,b]

[a] College of Environmental Science and Engineering, South China University of Technology, Guangzhou 510006, PR China
[b] The Key Lab of Pollution Control and Ecosystem Restoration in Industry Clusters, Ministry of Education, Guangzhou 510006, PR China
[c] The Key Laboratory of Environmental Protection and Eco-Remediation of Guangdong Regular Higher Education Institutions, PR China

ARTICLE INFO

Article history:
Received 19 April 2010
Received in revised form 3 July 2010
Accepted 6 July 2010

Keywords:
Cr(VI)
Montmorillonite
Pillared clays
Characterization
Adsorption isotherm

ABSTRACT

Four kinds of pillared montmorillonites were prepared by intercalating poly-hydroxyl iron, poly-hydroxyl iron/zirconium with different Fe/Zr molar ratios (4/1, 1/1) and poly-hydroxyl zirconium into the interlayer space of sodium-saturated montmorillonite (Na-Mt) via ion-exchange, termed Fe-Mt, $Fe/Zr_{4:1}$-Mt, $Fe/Zr_{1:1}$-Mt and Zr-Mt, respectively. The obtained materials were characterized by X-ray fluorescence (XRF) spectra, X-ray diffraction (XRD) spectra, Fourier transform infrared (FTIR) spectra, point of zero charge measurement and BET analysis. Batch experiments were conducted to investigate the adsorption behavior of Cr(VI) on selected samples. The results showed that the equilibrium uptake of Cr(VI) was highly pH-dependent with an optimal pH range of 3.0–6.0. The kinetics of Cr(VI) adsorption could be described well by the Pseudo-second-order model. The Langmuir adsorption isotherm provided the best correlation of the equilibrium data, and the estimated maximum equilibrium uptake of Cr(VI) of $Fe/Zr_{4:1}$-Mt was 22.35 mg/g at pH 3.0, 25 °C, higher than those of other three samples. Also, the thermodynamic parameters demonstrated that the process of Cr(VI) adsorption onto pillared montmorillonites was spontaneous and exothermic in nature. The presence of phosphate, sulphate and tartrate inhibited markedly the adsorption of Cr(VI), whereas nitrate, chlorate and acetate exhibited no significant effect on Cr(VI) adsorption. The analyses combining characterization results with adsorption data revealed that the removal mechanisms of Cr(VI) by these pillared montmorillonites mainly involved electrostatic interaction and ion-exchange. Overall, the regeneration of Fe/Zr-Mt could be achieved using NaOH solution, enabling a promising application for removing Cr(VI) from aqueous solution.

1. Introduction

The removal of heavy metals (e.g., Cd, Pb, Cr, Hg and As) from both natural water supplies and industrial wastewater is receiving an increasingly wide publicity because of their potential threats to plants, animals and human health. As known, hexavalent chromium [Cr(VI)], mainly arising from various industries including mining operation, metal plating, leather tanning, water cooling, and pigment manufacturing [1], is toxic and carcinogenic, and can cause health problems such as liver damage, pulmonary congestions, vomiting, and severe diarrhea [2]. Especially in some developing countries, people in the countryside almost rely on the groundwater for drinking, which is easily polluted by the industrial effluents around. Therefore, the release of Cr(VI)-containing wastewater should be strictly controlled to reduce the bad effect on biological systems.

Numerous methods have been developed for the treatment for Cr(VI)-rich effluents including chemical precipitation, membrane filtration, ion-exchange, reverse osmosis and commercial activated carbon adsorption [1,3,4], etc., but the sophisticated operation or relatively high cost is the main problem of these conventional techniques. Among alternative methods, adsorption is generally considered as an economical and effective method for removing contaminants like heavy metals especially combined with appropriate regeneration steps [5]. Hence, a variety of low-cost adsorbents for the removal of Cr(VI) have been reported such as spent clay [6], sand soil [7], layered double hydroxides [8,9] and agricultural waste products [10–12], etc. Notably, the montmorillonite, a 2:1 layered silicate clay mineral, has been extensively investigated in the field of environmental remediation for decades, owing to its high cation exchange capacity, large surface area, low cost and ready availability. Although the raw montmorillonite, for

* Corresponding author at: College of Environmental Science and Engineering, South China University of Technology, University Town, Guangzhou 510006, PR China. Tel.: +86 20 39380538; fax: +86 20 39383725.
E-mail address: pppxwu@scut.edu.cn (P. Wu).

1385-8947/$ – see front matter © 2010 Elsevier B.V. All rights reserved.
doi:10.1016/j.cej.2010.07.016

the permanent negative charge on the surface, shows hardly affinity to anion ions like Cr(VI), the interlayer cations (e.g., Na^+, K^+ and Ca^{2+}) can be replaced by various substances such as cationic surfactants and polymeric metal species. Thus, desirable physicochemical properties can be introduced into the material. In the recent years, much research on surfactant modified zeolites or montmorillontes for the removal of Cr(VI) from water has been reported [13–16]. Given its large surface area, high reactivity and positive charges, the inorganic pillared montmorillonite may be particularly suitable to be applied as an adsorbent for the treatment of Cr(VI)-containing wastewater, to which little attention has been paid.

Currently, much research interest for inorganic pillared montmorillonites has been directed towards mixed metal polycations pillared ones due to more superior porosities [17], thermal stabilities and catalytic activities [18], since the work on single metal pillars (e.g., Al, Zr, Fe and Cr) was well documented in previous studies [19–22]. The primary focus was on the use of these materials as catalysts [18,23,24], whereas their adsorption properties received less attention. Actually, Guerra et al. [25] discovered that Al/Ti and Al/Zr pillared clays were effective in the removal of zinc from water. Tian et al. [26] also found that Al/La pillared Mt performed better than Al-Mt in removing phosphate from solution. During the last few decades, a great of attention has been devoted to the pillared clays with mixed Al/M pillars, where M could be Fe, Cr, Zr, Ti or La, etc. [17,18,24–27], because of the well-defined chemical composition, structure and charge of Al_{13} species [28]. However, more information about other types of mixed metal pillars is necessary, and thus this study focuses on the mixed Fe/Zr pillars.

The nature of the pillars is very important and its choice depends upon the final target application. The Fe pillared montmorillonite (Mt) has attracted much attention due to its intrinsic catalytic activity and excellent adsorption performance [29], as reported in our previous studies [30,31]. Again, polymeric Fe species are the most effective coagulants or adsorption reagents for removing various impurities in potable water treatment [32] and possess high positive charges in comparison with polymeric Al species [33]. Furthermore, Cooper et al. [17] found that polymeric Fe modified Mt exhibited higher affinity towards metal ions than polymeric Al modified one. Yet many attempts to intercalate polymeric Fe species into Mt yielded products with relatively small basal spacings [29,30], which could result in an adverse impact on their surface areas and porous properties, and thus reduce their reaction activities. On the other hand, poly-hydroxyl zirconium is one of the most profusely used pillars [20], whose structure is $[Zr_4(OH)_{14}(H_2O)_{10}]^{2+}$. The Zr pillared Mt usually has a large basal spacing and microporous structure, and shows better thermal stability and performance of adsorption for organic compounds and metals than Al pillared one [34], although the chemistry of zirconium in aqueous medium and the factors ruling the species in equilibrium appear somewhat more constraining than for aluminum [24]. Consequently, the incorporation of the mixed Fe/Zr hydroxypolycations with the raw montmorillonite is expected to produce an advanced and promising material with developed porosity structure and more reactive sites such as hydroxyl groups (–OH). Heylen and Vansant [35] reported that mixed Fe/Zr pillared clay produced a different enhanced porosity supported by higher adsorption capacity towards CCl_4, $CHCl_3$, CH_2Cl_2 and CH_4 in contrast with Fe pillared clay. In this work, the detailed surface and structural properties of the polymeric Fe/Zr species pillared montmorillonite were studied, as well as its application for the removal of Cr(VI) from aqueous solution, about which, to our knowledge, no reports could be found in literatures.

In the present study, Fe/Zr pillared montmorillonites (Fe/Zr-Mts), Fe pillared montmorillonite (Fe-Mt) and Zr pillared montmorillonite (Zr-Mt) were prepared and further used for removing Cr(VI) from water to evaluate their feasibilities of application as adsorbents in the environmental remediation. The synthetic materials were studied through a combined analysis of XRF, BET, XRD, FTIR and zeta potential techniques. Furthermore, the experimental conditions including pH, temperature and coexisting anions were evaluated. Adsorption kinetics, equilibrium isotherms as well as thermodynamics were also investigated to establish the adsorption rates, maximum capacities and possible mechanisms of Cr(VI) adsorption onto pillared Mts.

2. Materials and methods

2.1. Material

Raw calcium montmorillonite (Ca-Mt), obtained from Nanhai, Guangdong province, China, has a cation exchange capacity (CEC) of 78.3 mmol/100 g and a basal spacing (d_{001}) of 1.56 nm. The sodium-saturated montmorillonite (Na-Mt) was prepared by ion-exchange reaction between Ca-Mt and NaCl, following a common procedure previously described [33]. All chemicals used in this study, e.g., NaCl, Na_2CO_3, $FeCl_3{\cdot}6H_2O$, $ZrOCl_2{\cdot}8H_2O$, KNO_3, $K_2Cr_2O_7$, HCl and NaOH were of analytical reagent grade, purchased from Guangzhou chemical reagent factory (Guangdong Province, China). The stock solution of 1000 mg/L Cr(VI) was prepared by dissolving potassium chromate in deionized water.

2.2. Preparation of adsorbents

2.2.1. Preparation of pillars

The Fe pillaring solution was synthesized as follows: 100 mL of Na_2CO_3 (0.1 mol) solution was added dropwise into the $FeCl_3$ (0.1 mol) solution under vigorous magnetic stirring through a separating funnel at a constant dropping rate of about 5 mL/min. After continuous stirring for 2 h, the resultant solution was aged for 24 h for further use. The experimental condition of water bath at 60 °C was maintained during the entire preparation process.

The Zr pillaring solution was prepared by adding $ZrOCl_2{\cdot}8H_2O$ powder (0.1 mol) into 250 mL deionized water (0.4 mol/L), followed by the same procedure as the above final part [24,25].

The mixed Fe/Zr pillaring solutions with different molar ratios of Fe/Zr were obtained by the following steps: the Fe pillaring solution was dropped into the Zr pillaring solution slowly under stirring, accompanied by a 3-h reaction.

2.2.2. Preparation of intercalated montmorillonites

The pillaring solution (namely Fe, $Fe/Zr_{4:1}$, $Fe/Zr_{1:1}$ or Zr) was added at a constant dropping rate of about 10 mL/min into Na-Mt suspension (2 wt.% of clay) under vigorous stirring to obtain a ratio of total metal/clay = 10 mmol/g. In order to improve the dispersion of the Na-Mt suspension, the suspension was pretreated by 15-min ultrasonic wave and 12-h continuous stirring prior to the above procedure. Afterwards, the mixture was kept stirring for 3 h and aged for 24 h. Finally, the solid was separated by centrifugation at 4000 rpm for 5 min, washed out the excess of pillaring agent on the surface with deionized water for several times, until free of chlorides, as indicated by the $AgNO_3$ test, air-dried at 80 °C, and pulverized to pass through a 200-mesh sieve. We referred to all synthetic samples as Fe-Mt, $Fe/Zr_{4:1}$-Mt, $Fe/Zr_{1:1}$-Mt and Zr-Mt, respectively.

2.3. Characterization of adsorbents

The chemical compositions of all materials were analyzed by a PANalytical PW-4400 X-ray fluorescence spectrometer (XRF).

The zeta potential values of the suspensions of prepared materials at different pH values were obtained to determine the points

Table 1
Elemental analysis of original montmorillonites and pillared clay samples.

Sample	O (%)	Si (%)	Al (%)	Mg (%)	Ca (%)	K (%)	Na (%)	Fe (%)	Zr (%)
Ca-Mt	50.8	32.4	6.75	1.86	1.7	0.09	0.72	2.07	–
Na-Mt	48.08	33.07	7.73	2.22	0.38	0.11	3.68	1.28	–
Fe-Mt	39.7	18.47	4.23	1.24	0.02	0.03	0.03	32.54	–
Fe/$Zr_{4:1}$-Mt	40.64	20.89	4.49	1.29	0.03	0.05	0.07	17.73	10.37
Fe/$Zr_{1:1}$-Mt	40.96	22.25	5.17	1.45	0.03	0.06	0.09	10.61	15.12
Zr-Mt	40.41	21.07	5.42	1.67	0.05	0.1	0.04	1.05	27.35

of zero charge (pH_{zpc}) using a Zetasizer (Malvern Instruments, UK) [6,36].

Nitrogen adsorption–desorption isotherms were measured using the ASAP 2020 volumetric adsorption analyzer. The samples were degassed at 423 K for 8 h. The specific surface area, S_{BET} of the sample was calculated by the BET method, and the total pore volume, V_t was obtained at a relative pressure of 0.9746. The *t*-plot method was used to calculate the micropore area, S_{micro}, external surface area, S_{ext}, and micropore volume, V_{micro}.

The X-ray powder diffraction (XRD) patterns of the samples were obtained by a Rigaku D/max-III diffractometer, equipped with Cu Kα radiation at 40 kV and 20 mA. All samples were recorded from 2° to 65° (2θ) at a scanning rate of 4°/min.

The Fourier transform infrared (FTIR) spectra of each sample were recorded between 400 cm^{-1} and 4000 cm^{-1} by the KBr pellet technique on a PerkinElmer 1725X Fourier transform infrared spectrometer.

2.4. Batch adsorption experiments

The adsorption behavior of Cr(VI) onto all samples was investigated through a batch method. 50 mg of a given adsorbent was weighed into a 50-mL glass bottle, followed by addition of 25 mL of Cr(VI) solution (25 mg/L), resulting in an adsorbent loading of 2 g/L. All reactors were placed in an oscillator at a rate of 200 rpm in a bath water of 25 ± 1 °C. Furthermore, the solution pH was fixed as 3.0 using 0.1 M HCl and 0.1 M NaOH, and all Cr(VI) solutions had a matrix of 0.05 M KNO_3 to keep the ionic strength relatively constant, unless noted.

The experiments for adsorption kinetics of Cr(VI) were conducted to determine both the rates of adsorption and the equilibrium times with the contact time ranging from 1 min to 720 min.

The effect of initial solution pH on Cr(VI) adsorption by the pillared samples was evaluated in the pH range of 1.0–10.0. In addition, to assess the stabilities of Fe and Zr loaded on these adsorbents, 50 mg of Fe/$Zr_{4:1}$-Mt was added into several bottles with 25 mL of deionized water, followed by the same procedure as the above. The concentrations of Fe and Zr in the solutions were measured using Hitachi Z-2000 AAS.

The adsorption isotherms were obtained at various temperatures (i.e., 25 °C, 35 °C, and 45 °C) and the initial concentration of Cr(VI) varied from 10 mg/L to 120 mg/L. After adsorption equilibrium, the suspension solutions were filtered via 0.45 μm fiber glass membranes and the filtrates were analyzed for the residual Cr(VI) concentrations by a Shimadzu 2501 PC UV–vis spectrophotometer according to the method described in the literature [15]. The amount of Cr(VI) adsorbed per unit mass the adsorbent, q_e (mg/g), was calculated as follows:

$$q_e = \frac{(c_0 - c_e)v}{m} \quad (1)$$

where c_0 and c_e (mg/L) are the initial and equilibrium concentrations, v is the volume of the solution (L), and m is the amount of adsorbent added (g).

The effect of some common coexisting anions in wastewater on Cr(VI) adsorption was determined by adding various anions such as phosphate, nitrate, sulphate, chlorate, acetate and tartrate into Cr(VI) solutions (50 mg/L) separately. The concentrations of these anions were all 1.0 mmol/L and other conditions were kept constant.

For the regeneration of Fe/$Zr_{4:1}$-Mt, 0.8 g of the adsorbent was mixed with 400 mL of Cr(VI) solution (50 mg/L) until adsorption equilibrium was reached. The solid was separated by centrifugation, and then immersed in the 0.1 M NaOH solution for 24 h to desorb Cr(VI) ions. Afterwards, the obtained solid was reused to adsorb Cr(VI). The above experimental operation was conducted over several cycles.

3. Results and discussion

3.1. Surface and textural properties analyses of synthetic materials

Elemental analysis of original montmorillonite (Mt) and pillared montmorillonites (Mts) by XRF is shown in Table 1. For synthetic samples, the lower contents of K, Ca and Na demonstrate that Fe, Zr or Fe/Zr pillars have entered into the interlaminar zone of Na-Mt via ion-exchange, which is further confirmed by the presence of iron and/or zirconium in these pillared Mts.

The pH_{zpc} values of all materials were determined by plotting the zeta potential values of the particulates suspension solutions (2 g/L) versus pH (Fig. 1) [6]. The pillaring step places a prominent influence on the surface property of Na-Mt. The zeta potential values for Na-Mt are constantly negative in the whole pH range, indicating its highly negatively charged surface. In sharp contrast, the points of zero charge for pillared samples increase significantly (Table 2), reflecting that positive charges have been introduced

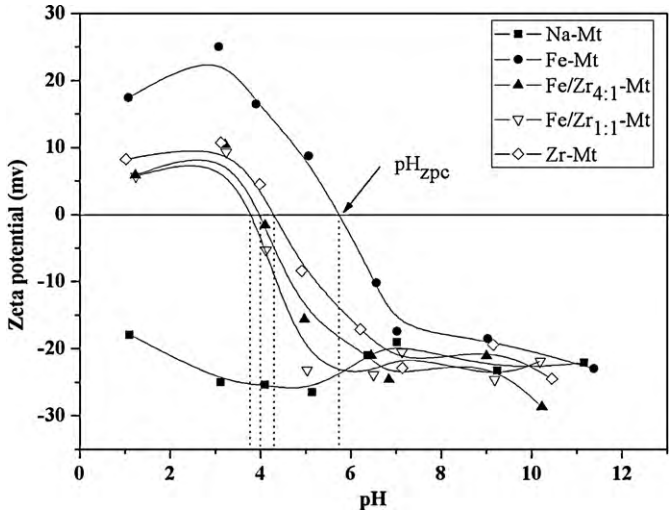

Fig. 1. Zeta potential values as a function of pH for all samples (2 g/L clay suspension).

Table 2
Point of zero charge, basal spacing and structural data of Na-Mt and pillared clay samples (S_{ext}, external surface area; S_{micro}, microporous surface area, evaluated from *t*-plot; D_a, average pore diameter; V_t, total porous volume; V_{micro}, microporous volume).

Sample	pH_{zpc}	d_{001} (nm)	S_{BET} (m^2/g)	S_{ext} (m^2/g)	S_{micro} (m^2/g)	D_a (nm)	V_t (cm^3/g)	V_{micro} (cm^3/g)
Na-Mt	–	1.27	80.2433	57.0050	23.2438	7.9684	0.2059	0.010358
Fe-Mt	5.8	1.58	163.800	156.142	7.65880	7.0805	0.2983	0.001823
$Fe/Zr_{4:1}$-Mt	4.0	1.83	145.173	92.0570	53.1164	5.6102	0.1987	0.023950
$Fe/Zr_{1:1}$-Mt	3.8	2.01	121.632	63.8010	57.8300	5.5001	0.1835	0.026415
Zr-Mt	4.3	2.01	176.942	71.3900	105.552	3.8493	0.1621	0.048548

into Na-Mt. In addition, it is interesting to note that the pH_{zpc} values of Fe/Zr-Mts ($Fe/Zr_{4:1}$-Mt and $Fe/Zr_{1:1}$-Mt) are lower than those of both Fe-Mt and Zr-Mt. This fact could be illustrated like that the mixed Fe/Zr polyoxycations, presumably present as $\{[Fe_xZr_y(OH)_z(H_2O)_n]^{(3x+4y-z)+}\}$, on the surfaces of Fe/Zr-Mts could combine more hydroxyl groups (–OH) and thus bring about lower positive charges and sequent lower pH_{zpc} values.

The porous structural data of Na-Mt and intercalated samples are included in Table 2. As expected, all samples display a high specific surface area comparing to Na-Mt (80.23 m^2/g). Fe-Mt exhibits smaller micropore surface area (7.6588 m^2/g) and micropore volume (0.001823 cm^3/g) than those of Na-Mt. Similar result was also reported by Heylen and Vansant [35]. Unlike their result, in the present work, a small d_{001} (1.58 nm) and a large external surface area (156.14 m^2/g) were also observed. A reasonable interpretation is that only some small-sized Fe species could enter into the interlayer region, which obstructed some of the main channels of Na-Mt, and simultaneously, new mesopores were formed within iron hydroxide clusters on the external surface of Fe-Mt [37]. In contrast, for $Fe/Zr_{4:1}$-Mt, $Fe/Zr_{1:1}$-Mt and Zr-Mt, the volume of micropores relative to that of Na-Mt significantly increases with increasing zirconium content, suggesting that the incorporation of zirconium species make a positive impact on the microporous structure of pillared Mts.

3.2. XRD and FTIR analyses of all samples

Shown in Fig. 2 are the XRD patterns of all samples in the low 2θ angle region. Compared with the d_{001} (1.27 nm) of Na-Mt, the basal spacings (d_{001}) increase by 0.31 nm, 0.56 nm, 0.74 nm and 0.74 nm for Fe-Mt, $Fe/Zr_{4:1}$-Mt, $Fe/Zr_{1:1}$-Mt and Zr-Mt, respectively. These changes reveal that Fe, Zr or Fe/Zr pillars have been intercalated into the interlayer space of Na-Mt. Meanwhile a clear trend can be observed that the d_{001} increases with the decrease in Fe contents among the synthetic materials. This is because Fe species mainly distribute on the external surface, while more Zr or mixed Fe/Zr species are inserted into the interlayer region. This result matches well with the BET analysis result and some previous studies [30,38]. What is more, the basal spacings of Fe-Mt, $Fe/Zr_{1:1}$-Mt, and Zr-Mt decrease by 0.06 nm, 0.08 nm and 0.06 nm, respectively, after Cr(VI) adsorption. It is well-known that the basal spacings of clay minerals are closely relative with the adsorbed water content in the interlayer region [39]. Accordingly, this result implies that the adsorption of Cr(VI) may cause the decrease of the interlayer water content.

Fig. 3 shows the FTIR spectra (400–4000 cm^{-1}) of all materials. The wavenumbers and assignments of main vibration peaks are listed in Table 3, referring to previous reports [20,29,40]. The broad appearances around 3440 cm^{-1} corresponding to O–H stretching mode of adsorbed water shift to the lower wavenumbers (Table 3) with a simultaneous increase in the width, demonstrating an increase in interlayer water content due to the replacement of inorganic cations with the metal pillars [40]. Besides, significant decreases of the peaks at near 3628 cm^{-1} and in the range of 400–1090 cm^{-1}, are detected for all pillared Mts, suggesting that the Fe, Zr or Fe/Zr mixed polyoxocations could link with Al–O in the alumina octahedral sheet and Si–O in the silica tetrahedron plates [41]. The FTIR spectra (not shown) of Fe-Mt, $Fe/Zr_{1:1}$-Mt and Zr-Mt after adsorbing chromate ions show that the adsorption of Cr(VI) has resulted in significant decreases of the bands near 3440 cm^{-1} and 1650 cm^{-1}, which means a decrease of water content in the interlayer space, in agreement with the analysis of XRD result.

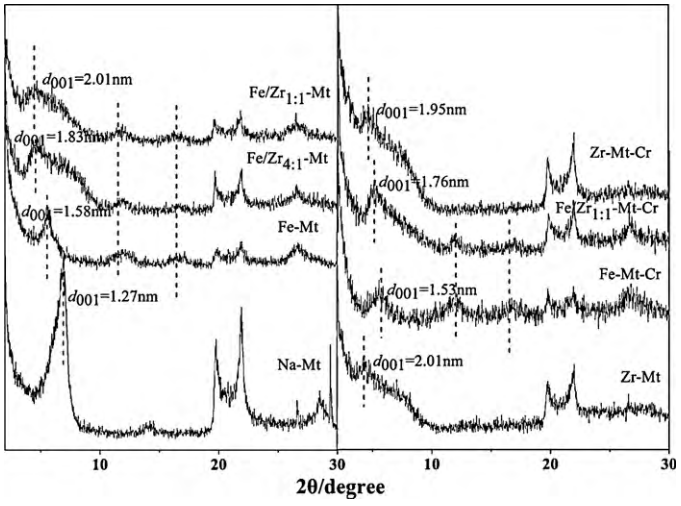

Fig. 2. X-ray patterns of Na-Mt and pillared samples before and after the adsorption of Cr(VI).

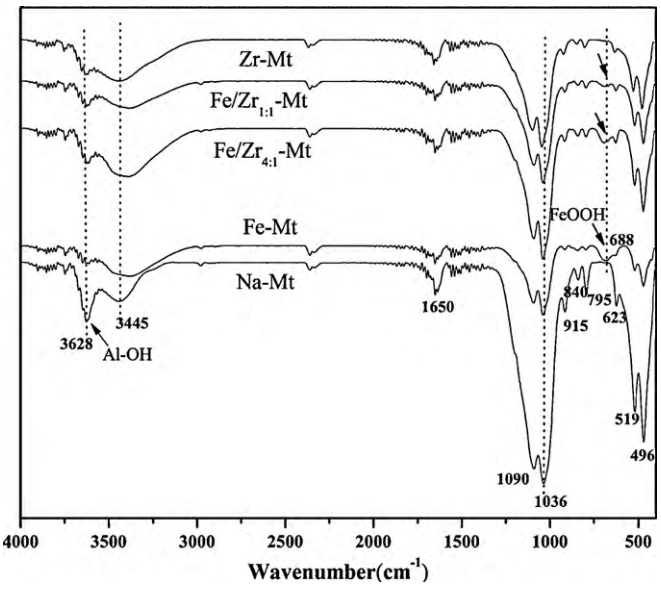

Fig. 3. Infrared spectra of all samples (Na-Mt, Fe-Mt, $Fe/Zr_{4:1}$-Mt, $Fe/Zr_{1:1}$-Mt and Zr-Mt).

Table 3
Positions (cm^{-1}) and assignments of main IR vibration bands for all samples before and after the adsorption of Cr(VI).

Sample	Stretching and deformation of Al–OH		Stretching and deformation of OH of water		Stretching of Si–O		Deformation of Al–Mg–OH	Deformation of FeOOH	Deformation of Si–O			
Na-Mt	3628	915	3445	1650	1090	1036	840	–	795	623	519	469
Fe-Mt	3629	915	3387	1650	1091	1039	844	688	795	624	519	469
Fe/$Zr_{4:1}$-Mt	3628	915	3393	1650	1091	1038	841	693	795	626	519	470
Fe/$Zr_{1:1}$-Mt	3629	915	3386	1650	1089	1039	839	687	795	625	519	469
Zr-Mt	3628	915	3411	1650	1090	1038	839	–	795	626	519	469
Fe-Mt-Cr	3629	915	3418	1650	1090	1038	842	691	795	626	519	469
Fe/$Zr_{1:1}$-Mt-Cr	3628	914	3420	1650	1088	1040	841	690	795	625	519	470
Zr-Mt-Cr	3627	916	3420	1643	1087	1039	840	–	795	624	520	470

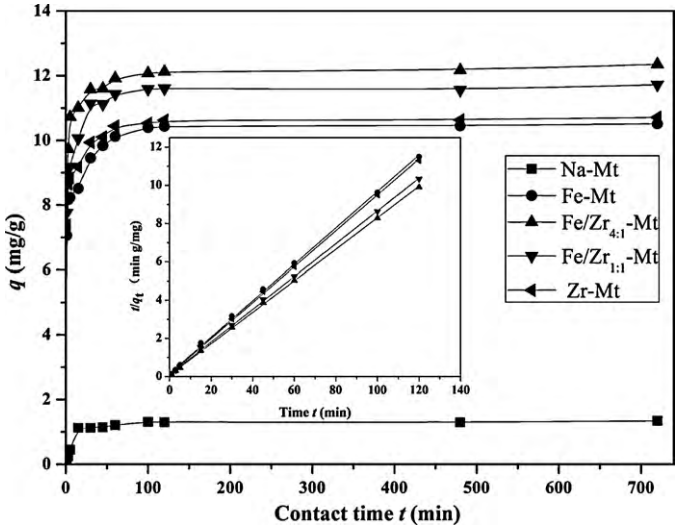

Fig. 4. Effect of contact time on the adsorption of Cr(VI) by Na-Mt and pillared samples, and Pseudo-second-order linear plot (inset) (experimental conditions: 25 mg/L Cr(VI), adsorbent dose 2 g/L, pH 3.0, ionic strength 0.05 M, temperature 25 °C).

3.3. Effect of contact time and kinetics study

As demonstrated by the observed Cr(VI) uptake versus t profile (Fig. 4), the pillared clays displayed quite high removal rates and efficiencies (83–97%), whereas Na-Mt was almost invalid, in accordance with the previous report [42]. So Na-Mt was not selected for further experiments. As seen in Fig. 6, at the beginning, all adsorption processes were very fast, especially for Fe/$Zr_{4:1}$-Mt, then progressed and plateaued within 120 min. Hence, a contact time of 2 h was adopted to study the adsorption equilibrium. Taking Fe/$Zr_{4:1}$-Mt for example, about 88% and 96% of Cr(VI) uptake were achieved within 15 min and 60 min, respectively, while only a small part of the additional uptake occurred during the rest reaction time.

To understand the mechanism of the adsorption process, several rate models were used to analyze the experimental data including the Pseudo-first-order (2), Pseudo-second-order (3) and Elovich equation (4) models [33]. The linear forms of the above models could be expressed as

$$\ln(q_e - q_t) = \ln\ q_e - k_1 t \quad (2)$$

$$\frac{t}{q_t} = \frac{1}{k_2 q_e^2} + \frac{1}{q_e} t \quad (3)$$

$$q_t = \frac{1}{\beta}\ \ln(\alpha\beta) + \frac{1}{\beta}\ln t \quad (4)$$

where q_t (mg/g) and q_e (mg/g) are the amounts of Cr(VI) adsorbed at time t (min) and at equilibrium, respectively; k_1 and k_2 are the sorption rate constants of the Pseudo-first-order equation and Pseudo-second-order equation, respectively; α is the initial adsorption rate and β is related to surface coverage and activation energy of chemisorptions.

Table 4 summarizes the corresponding models fitting parameters. For the Pseudo-second-order model, the coefficients of determination (R^2) are very high, above 0.999 and the values of the theoretical q_e for all pillared samples are in good agreement with the experimental q_e values in comparison with the Pseudo-first-order model. Accordingly, the Pseudo-second-order model is the most likely to describe the kinetics over the whole adsorption process, implying that the rate-limiting step may be a chemical sorption [42].

The linear plots of the Pseudo-second-order model are shown in the inset of Fig. 4. As mentioned above, both k_2 and α represent the adsorption rate in the fast adsorption stage. In the case of Fe/$Zr_{4:1}$-Mt, k_2 is 7.3×10^{-2} g/(mg min) and particularly, the value of α is 1.1×10^6 mg/(g min), 1–2 orders of magnitude larger than those of other materials, suggesting that the adsorption of Cr(VI) onto Fe/$Zr_{4:1}$-Mt is the fastest among all samples, also much faster than that of Cr(VI) on HDTMAB-Mt [43]. The highest rate for Fe/$Zr_{4:1}$-Mt indicates that there are more easily accessible adsorption sites on its exterior or interior surfaces compared with other samples, thus giving rise to a rapid equilibrium.

3.4. Effect of initial solution pH

The effect of solution pH on Cr(VI) adsorption by the pillared Mts was evaluated in batch systems over a pH range of 1.0–10.0 (Fig. 5). It was evident that the removal of Cr(VI) by the adsorbents was highly pH-dependent. Sharp decreases of adsorption capacity for all pillared clays occurred over the initial pH range of 6.0–10.0. The uptakes of Cr(VI) onto Fe-Mt, Fe/$Zr_{4:1}$-Mt and

Table 4
Kinetics parameters for Cr(VI) adsorption onto pillared montmorillonites.

Sample	$q_{e\,(experiment)}$ (mg/g)	Pseudo-first-order model			Pseudo-second-order model			Elovich model		
		k_1 (min^{-1})	q_e (mg/g)	R^2	k_2 [g/(mg min)]	q_e (mg/g)	R^2	α [mg/(g min)]	β (g min^2/mg)	R^2
Fe-Mt	10.435	0.044	3.988	0.964	0.046	10.552	0.999	1.8×10^4	1.429	0.984
Fe/$Z_{4:1}$-Mt	12.12	0.045	3.241	0.937	0.073	12.185	0.999	1.1×10^6	1.557	0.980
Fe/$Zr_{1:1}$-Mt	11.61	0.056	4.272	0.972	0.059	11.721	0.999	1.6×10^4	1.238	0.985
Zr-Mt	10.62	0.042	3.179	0.936	0.064	10.686	0.999	9.6×10^4	1.550	0.985

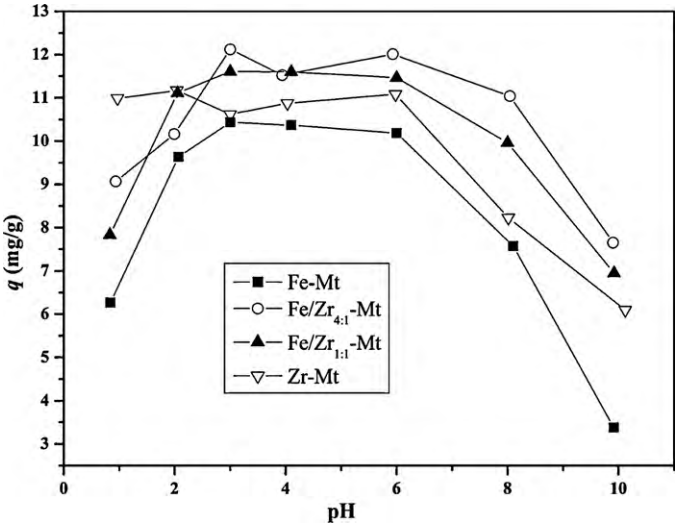

Fig. 5. Effect of initial solution pH on the adsorption of Cr(VI) by Fe-Mt, $Fe/Zr_{4:1}$-Mt, $Fe/Zr_{1:1}$-Mt and Zr-Mt (experimental conditions: 25 mg/L Cr(VI), adsorbent dose 2 g/L, contact time 2 h, ionic strength 0.05 M, temperature 25 °C).

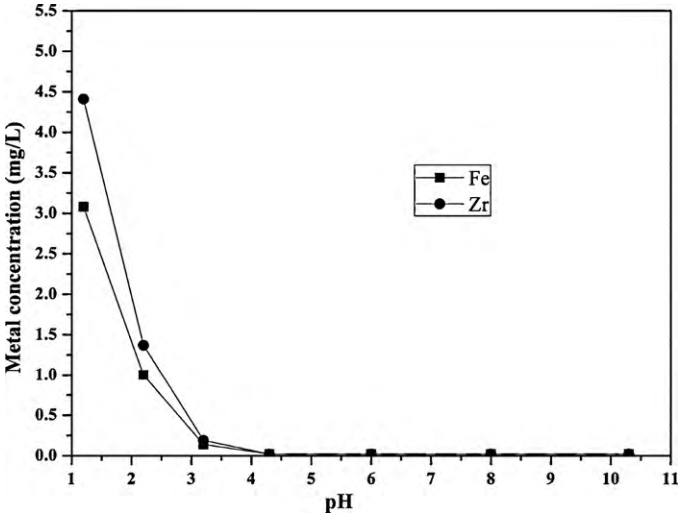

Fig. 6. The concentrations of released Fe and Zr ions in solution at various pH.

$Fe/Zr_{1:1}$-Mt offered quite similar pH-dependency, with an optimal pH range of 3.0–6.0. It was noteworthy that abrupt decreases were observed for $Fe/Zr_{4:1}$-Mt, $Fe/Zr_{1:1}$-Mt and Fe-Mt when pH came to below ~3.0, whereas Zr-Mt exhibited a relatively stable and efficient uptake of Cr(VI) in the pH range of 1.0–6.0. For instance, the maximum adsorption capacity of $Fe/Zr_{4:1}$-Mt occurred at pH 3 and diminished 3.1 mg/g and 4.5 mg/g decreasing pH from 3.0 to 1.0 and increasing pH from 3.0 to 10.0, respectively.

According to the distribution diagram of Cr(VI) species as a function of pH [6], In the pH range of 1.0–6.0, the predominant species exists as $HCrO_4^-$ and above pH 6.0 as $Cr_2O_4^{2-}$. The pH_{zpc} values of the pillared clays are between 3.8 and 5.8, that is, these adsorbents surfaces are negatively charged at pH > 6.0. Hence, an increasing pH causes the surfaces to carry more negative charges and results in stronger electrostatic repulsion to $Cr_2O_4^{2-}$, a more negatively charged species, blocking the adsorption processes. Also, the adsorption processes are further hindered because of the competitive adsorption between OH^- with $Cr_2O_4^{2-}$ [26,42]. In contrast, at lower pH, protons (H^+) adsorbed on the surfaces of these clays bring about more positive charges and thus enhance the electrostatic attraction between the surfaces and negatively charged Cr(VI) anions. But the dramatic decreases of Cr(VI) uptake from pH 3.0 to 1.0 for Fe-Mt and Fe/Zr-Mts could be attributed to the dehydroxylation of Fe or Fe/Zr hydroxypolycations as a result of acid–base neutralization. Similar phenomenon was also observed in the research [44]. However, the decrease of uptake for Zr-Mt is not as obvious as other samples, thus denoting the better stability of the intercalated Zr hydroxypolycations.

To assess the possible risk of metal leakage during the adsorption of Cr(VI), the releasing behavior of Fe and Zr was investigated by measuring the Fe and Zr concentrations in the solutions under different pH values (1.0–10.0). The result is shown in Fig. 6. We could see that the concentrations of Fe ions in the solutions at pH 2.0 and 3.2 are 1.0 mg/L and 0.14 mg/L, respectively. Especially when the solution pH is above 4.0, the Fe and Zr ions in the solutions are not nearly detected. So the risk of metal leakage resulting from the dissolution of the material is receivable in the optimum pH range.

Meanwhile, the decreases in the low pH range also reveal that the hydroxyls in hydroxypolycations play a key role in the adsorption process although there are high positive charges on the surfaces of the adsorbents indicated by Fig. 1. Besides, at pH > pH_{zpc} (4.0–6.0), Fe/Zr-Mts and Zr-Mt still exhibited efficient uptakes for Cr(VI) and the effect of pH on Cr(VI) retention was slight in the pH range of 3.0–6.0 for all the samples. Consequently, it can be inferred that the electrostatic interaction is not the only mechanism involved in the adsorption process. And we propose that the ion-exchange between Cr(VI) and hydroxyl (–OH) is more likely to describe the adsorption process, as presented conceptually by Eqs. (5) and (6) in the condition of pH < 6.0 (M mainly represents Fe, Zr, or mixed Fe/Zr), because the ion-exchange mechanism is much less dependent on pH than the electrostatic interaction [33]. Moreover, as the affinity of Cr(VI) with metal oxide is higher than that of hydroxide with metal oxide [45], the chromate ions can replace the hydroxide from the surface of the hydrolyzed metal oxides. Of course, the evaluation of effect of solution pH is just a macroscopic method of inferring mechanism, which can be further directly confirmed using microscopic methods such as X-ray adsorption near-edge structure spectrum.

$$M\text{–}OH + HCrO_4^- \rightarrow M\text{–}HCrO_4^- + OH^- \quad (5)$$

$$M\text{–}OH_2^+ + HCrO_4^- \rightarrow M\text{–}HCrO_4^- + H_2O \quad (6)$$

3.5. Effect of initial concentration and adsorption isotherms

Equilibrium relationships between adsorbate and adsorbent are described by adsorption isotherms. Fig. 7 shows the isotherms of the adsorption of Cr(VI) onto the pillared Mts. The Langmuir (7), Freundlich (8) and Temkin (10) isotherm models [5] were used to describe the equilibrium data, and their linear forms were presented as

$$\frac{c_e}{q_e} = \frac{1}{q_m k_L} + \frac{1}{q_m} c_e \quad (7)$$

$$\ln\ q_e = \ln k_F + \left(\frac{1}{n}\right) \ln c_e \quad (8)$$

$$q_e = \left(\frac{RT}{b_T}\right) \ln A_T + \left(\frac{RT}{b_T}\right) \ln c_e \quad (9)$$

where C_e (mg/L) is equilibrium concentration of Cr(VI) in the solution, q_e (mg/g) is the amount of Cr(VI) adsorbed at equilibrium, q_m (mg/g) is the theoretical maximum monolayer sorption capacity, k_L is a constant representing the affinity of the sorbent for the solute; the k_F and n are the indicators of the adsorption capacity and adsorption intensity, respectively; b_T is Temkin heat of sorption (kJ/mol), and A_T is Temkin adsorption potential (L/mg).

The linearized isotherms of Langmuir model are depicted in the inset of Fig. 7, and the adsorption constants (q_m, k_L, k_F, n, b_T, A_T

Table 5
Equilibrium isotherm model parameters for Cr(VI) adsorption onto pillared montmorillonites.

Sample	Langmuir			Freundlich			Temkin		
	k_L (L/mg)	q_m (mg/g)	R^2	$1/n$	k_F (L/g)	R^2	b_T (kJ/mol)	A_T (L/mg)	R^2
Fe-Mt	0.237	16.210	0.999	0.126	8.869	0.973	1.511	144.589	0.963
Fe/$Z_{4:1}$-Mt	0.396	22.346	0.995	0.131	12.477	0.989	1.136	272.751	0.981
Fe/$Zr_{1:1}$-Mt	0.378	21.115	0.996	0.134	11.680	0.966	1.154	190.039	0.972
Zr-Mt	0.337	19.238	0.997	0.148	10.053	0.915	1.131	72.201	0.936

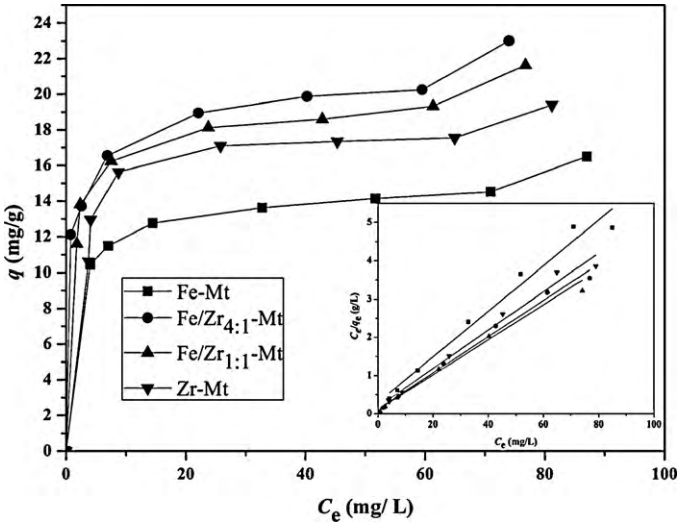

Fig. 7. Adsorption isotherms of Cr(VI) on Fe-Mt, Fe/$Zr_{4:1}$-Mt, Fe/$Zr_{1:1}$-Mt and Zr-Mt and Langmuir linear plot (inset) (experimental conditions: pH 3.0, adsorbent dose 2 g/L, contact time 2 h, ionic strength 0.05 M, temperature 25 °C).

and R^2) values are given in Table 5. As evidenced by the correction coefficient R^2, the Langmuir model could describe the adsorption process better than Freundlich and Temkin models with $R^2 > 0.99$. This result indicates that these pillared clays provide the specific homogeneous sites and the adsorption of Cr(VI) displays a monolayer adsorption process [36].

According to the values of q_m, k_L and k_F, the order of maximum adsorption capacities and affinities of the four materials to Cr(VI) is: Fe-Mt < Zr-Mt < Fe/$Zr_{1:1}$-Mt < Fe/$Zr_{4:1}$-Mt, showing that mixed metal pillars exhibit more superior activities compared to single metal pillars, as supported by the previous reports [17,26,33]. As discussed above, Fe-Mt and Zr-Mt have larger surface areas and higher surface positive charges but smaller maximum capacities than Fe/Zr-Mts, demonstrating that the adsorption of Cr(VI) is not controlled by a physical sorption process. This could be interpreted as follows: the mixed Fe/Zr polyoxocations could combine more hydroxyl groups and the adsorption process is mainly determined by the ion-exchange reaction between chromate ions and hydroxyls. And therefore, there are more active adsorption sites on the surfaces of Fe/Zr-Mts, resulting in higher adsorption capacities. This interpretation is supported by the results in 3.1 and 3.4. Further, the ion-exchange reaction between Cr(VI) and hydroxyls may reduce the bond intensity between hydroxypolycations and combined water and thus give rise to the decrease of water content after adsorbing Cr(VI), which is also evidenced by the results of XRD and FTIR. Nevertheless, it must be emphasized that the electrostatic attraction exerts a positive impact on the adsorption of Cr(VI) although it is not a decisive factor of Cr(VI) removal. To be specific, the ion-exchange process could be enhanced by electrostatic attraction but also hindered by electrostatic repulsion as revealed by the decreasing uptakes of Cr(VI) in the pH range of 6.0–10.0.

The maximum adsorption capacities obtained from the Langmuir model and equilibrium times of the pillared Mts are compared with those of other adsorbents investigated for the removal of Cr(VI) under similar conditions reported in previous literatures (Table 6). We can see that the pillared Mts, especially Fe/Zr-Mt have a relatively short reaction time and acceptably high capacities for the removal of Cr(VI), suggesting promising potential for the treatment of Cr(VI)-rich wastewater.

3.6. Effect of temperature and thermodynamics study

The effect of temperature on the adsorption of Cr(VI) onto Fe-Mt, Fe/$Zr_{1:1}$-Mt and Zr-Mt was examined at 298 K, 308 K and 318 K. Fig. 8 shows that adsorption capacity decreased slightly with the increase in temperatures. For Fe/$Zr_{1:1}$-Mt, the maximum adsorption capacity q_m calculated from Langmuir model decreased from 21.11 mg/g at 298 K to 19.24 mg/g at 318 K. In order to further investigate the effect of temperature on the adsorption, thermodynamic parameters such as change in Gibbs free energy (ΔG), change in enthalpy (ΔH) and change in entropy (ΔS) were estimated using

Table 6
Comparison of adsorption capacity, q_m obtained from Langmuir equation of Cr(VI) on various adsorbents.

Adsorbents	Temperature (°C)	pH	Equilibrium time	q_m (mg/g)	References
Wollastonite	30	2.5	100 min	0.686	[49]
Spent activated clay	24	2.0	1.5 h	5.037	[6]
Organic-modified rectorite	25	6.0	40 min	3.57	[16]
HDTMA-modified zeolite	25	6.0	-	5.19	[15]
HDTMA-modified montmorillonite	25	4.2	-	23.3	[13]
Modified jacobsite ($MnFe_2O_4$)	25	4.0	5 min	22.68	[36]
Montmorillonite-supported magnetite	25	2.0	1 h	15.3	[42]
Modified bauxite tailings	25	5.0–6.0	3 h	1.399	[46]
Clarified sludge	30	3.0	2 h	26.31	[47]
Activated alumina	30	3.0	3 h	25.57	[47]
Activated carbon coated with quaternized poly (4-vinylpyridine)	24	2.25	9 h	53.7	[1]
Almod shell activated carbon	50	1.0	-	190.3	[10]
Hazelnut shell activated carbon	30	2.0	50 h	60.39	[11]
Fe pillared montmorillonite	25	3.0	2 h	16.21	In this study
Fe/$Zr_{4:1}$ pillared montmorillonite	25	3.0	2 h	22.34	In this study
Zr pillared montmorillonite	25	3.0	2 h	19.24	In this study

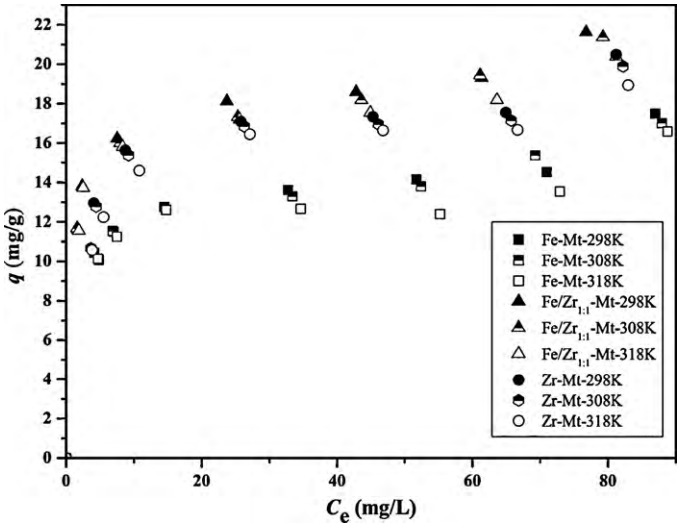

Fig. 8. Effect of temperature on the adsorption of Cr(VI) by Fe-Mt, Fe/$Zr_{1:1}$-Mt and Zr-Mt (experimental conditions: pH 3.0, adsorbent dose 2 g/L, contact time 2 h, ionic strength 0.05 M, Cr(VI) concentration 25–120 mg/L).

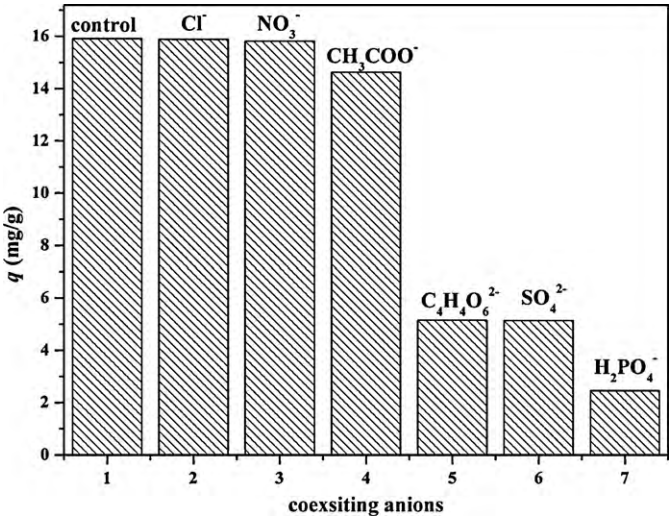

Fig. 9. Effect of coexisting anions on Cr(VI) adsorption by Fe/$Zr_{4:1}$-Mt (experimental conditions: pH 3.0, adsorbent dose 2 g/L, contact time 2 h, Cr(VI) concentration 50 mg/L, temperature 25 °C).

the following equations [47]:

$$k_D = \frac{q_e}{c_e} \tag{10}$$

$$\Delta G = -RT \ln k_D \tag{11}$$

$$\Delta G = \Delta H - T\Delta S \tag{12}$$

$$\ln k_D = \frac{\Delta S}{R} - \frac{\Delta H}{RT} \tag{13}$$

where k_D is the distribution coefficient (mL/g), R is gas law constant (8.314 J mol^{-1} K^{-1}) and T is the absolute temperature (K). ΔH and ΔS are obtained from the slope and intercept of Van't Hoff plots of $\ln k_D$ versus $1/T$. Thermodynamic parameters based on the above functions are listed in Table 7. The negative values of ΔG indicate the adsorption process is spontaneous, and the degree of spontaneity of the reaction increases with increasing temperature. We can see that enthalpy change ΔH values of Cr(VI) adsorption are also negative, which means all adsorption processes are exothermic in nature. The exothermic adsorption of Cr(VI) onto modified clays were also reported by other authors [16,43]. In addition, the positive values of ΔS indicate that there is an increase in the randomness in the system solid/solution interface during the adsorption process [48].

3.7. Effect of coexisting anions on Cr(VI) removal

The effect of coexisting anions, e.g., chlorate, nitrate, acetate, acetate, sulphate, and phosphate on the adsorption of Cr(VI) by Fe/$Zr_{4:1}$-Mt was investigated at a constant concentration level (1.0 mmol/L) for each anion (Fig. 9). The result showed that the anions such as Cl^-, NO_3^- almost exhibited no noticeable effect on the removal of Cr(VI). However, the coexisting $C_4H_4O_6^{2-}$, SO_4^{2-} and $H_2PO_4^-$ markedly inhibited the retention of Cr(VI). For example, the observed uptakes of Cr(VI) in the presence of SO_4^{2-} and $H_2PO_4^-$ were only 5.14 mg/g and 2.15 mg/g, respectively, compared with the adsorption density of 15.91 mg/g in the control. The reason responsible for the decrease of Cr(VI) adsorption could be contributed to the competition for the active surface sites of Fe/$Zr_{4:1}$-Mt. Overall, the effect of these coexisting anions followed the order: $H_2PO_4^- > SO_4^{2-} \approx C_4H_4O_6^{2-} > CH_3COO^- > NO_3^- \approx Cl^-$, reflecting their different affinities towards the active surface sites of the adsorbent.

Table 7
Thermodynamic parameters for Cr(VI) adsorption onto pillared montmorillonites at pH 3.0, 40 mg/L Cr(VI).

Sample	$-\Delta H$ (kJ/mol)	ΔS (J/mol K)	$-\Delta G$ (kJ/mol)		
			298 K	308 K	318 K
Fe-Mt	5.07	33.26	14.98	15.31	15.65
Fe/$Z_{4:1}$-Mt	6.34	34.67	16.67	17.02	17.37
Fe/$Zr_{1:1}$-Mt	5.10	37.92	16.4	16.78	17.16
Zr-Mt	3.47	42.41	16.1	16.53	16.69

3.8. Regeneration study of Fe/Zr-Mt

In order to reduce the cost of raw materials, the reuse of adsorbents must be taken into account in the application. Thus, it is important to find an efficient regeneration method to desorb Cr(VI) ions from the adsorbents. Previous studies have reported many regeneration ways for various anions such as using NaOH [26,36] and NaCl [44]. In this study, the regeneration of spent Fe/$Zr_{4:1}$-Mt was examined by using deionized water, NaCl and NaOH, respectively. The experimental results demonstrated the Cr(VI)

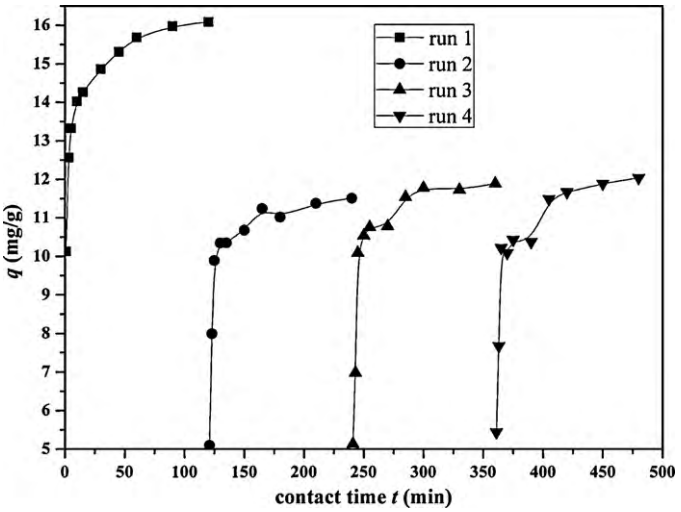

Fig. 10. Regeneration studies of Fe/$Zr_{4:1}$-Mt.

desorption hardly occurred in pure water and the desorption efficiencies in the 0.1 M NaOH solution and 10% NaCl solution were 82% and 35%, respectively. Therefore, we used NaOH solution to regenerate the spent Fe/$Zr_{4:1}$-Mt. Afterwards, the readsorption of Cr(VI) by the same adsorbent was conducted in three cycles. As indicated in Fig. 10, the adsorption capacity of Cr(VI) in the second run was by about 4.0 mg/g less than that in the first run, suggesting that there may be some irreversible sites on the surface of Fe/$Zr_{4:1}$-Mt. In the following runs, the uptake of Cr(VI) almost remained unchanged.

4. Conclusions

Pillared montmorillonites, i.e., Fe-Mt, Fe/$Zr_{4:1}$-Mt, Fe/$Zr_{1:1}$-Mt and Zr-Mt, were synthesized and applied to evaluate their feasibilities as adsorbents to remove Cr(VI) from solutions. The surface and structural properties of these obtained materials were improved remarkably when compared to original Na-Mt. The XRD patterns confirmed that the Fe, Zr and Fe/Zr pillars were intercalated into the interlayer space of Na-Mt and Fe species were mainly located on the external surfaces evidenced by the increasing d_{001} values. Also, the IR spectra demonstrated that these metal pillars linked with Al–O in the alumina octahedral sheet and Si–O in the silica tetrahedron plates. Furthermore, the synthetic samples exhibited larger specific surface areas and possessed higher positive charges on external surfaces as indicated by the results of BET and zeta potential measurement.

Adsorption experiments showed that the removal of Cr(VI) was rapid and the kinetics could be described well by the Pseudo-second-order model ($R^2 > 0.99$) with an equilibrium time of 2 h. The equilibrium studies indicated that solution pH exerted an important impact on the adsorption of Cr(VI) with an optimal pH range of 3.0–6.0. The Langmuir adsorption isotherm provided the best correlation of the equilibrium data. Thermodynamic parameters demonstrated that the adsorption process of Cr(VI) onto these pillared montmorillonites was spontaneous and exothermic in nature. The coexisting anions such as phosphate, sulphate and tartrate inhibited markedly the adsorption of Cr(VI), whereas nitrate, chlorate and acetate exhibited no significant effect on Cr(VI) adsorption. NaOH solution could be used to regenerate the spent adsorbents. Moreover, the combined results revealed that the adsorption of Cr(VI) was mainly governed by electrostatic attraction and ion-exchange, the latter of which played a major role.

These preliminary results indicate that Fe/Zr pillared montmorillonite can be applied as an effective adsorbent for the treatment of Cr(VI)-rich wastewater.

Acknowledgements

This work was financially supported by the Program for National Science Foundation of China (Grant No. 40973075, 40730741, and 40573064), New Century Excellent Talents Program, Ministry of Education, China (Grant No. NCET-06-0747), Science and Technology Plan of Guandong Province, China (Grant Nos. 2006B36601004, 2008B30302036, and 2009B050900005), Natural Science Foundation of Guangdong Province, China (Grant Nos. 06025666, 9351064101000001) and the Fundamental Research Funds for the Central Universities, SCUT (Grant Nos. 2009ZZ0048, 2009ZZ0073, and 2009ZM0202).

References

[1] J. Fang, Z.M. Gu, D.C. Gang, C.G. Liu, E.S. Ilton, B.L. Deng, Cr(VI) removal from aqueous solution by activated carbon coated with quaternized poly(4-vinylpyridine), Environ. Sci. Technol. 41 (2007) 4748–4753.
[2] C. Raji, T.S. Anirudhan, Batch Cr(VI) removal by polyacrylamide-grafted sawdust: kinetics and thermodynamics, Water Res. 32 (1998) 3772–3780.
[3] S.J. Park, Y.S. Jang, Pore structure and surface properties of chemically modified activated carbons for adsorption mechanism and rate of Cr(VI), J. Colloid Interface Sci. 249 (2002) 458–463.
[4] N.Q. Zhao, N. Wei, J.J. Li, Z.J. Qiao, J. Cui, F. He, Surface properties of chemically modified activated carbons for adsorption rate of Cr(VI), Chem. Eng. J. 115 (2005) 133–138.
[5] Y.H. Wu, B. Li, S.X. Feng, X.M. Mi, J.L. Jiang, Adsorption of Cr(VI) and As(III) on coaly activated carbon in single and binary systems, Desalination 249 (2009) 1067–1073.
[6] C.H. Weng, Y.C. Sharma, S.H. Chu, Adsorption of Cr(VI) from aqueous solutions by spent activated clay, J. Hazard. Mater. 155 (2008) 65–75.
[7] B. Fonseca, H. Maio, C. Quintelas, A. Teixeira, T. Tavares, Retention of Cr(VI) and Pb(II) on a loamy sand soil kinetics, equilibria and breakthrough, Chem. Eng. J. 152 (2009) 212–219.
[8] R.L. Goswamee, P. Sengupta, K.G. Bhattacharyya, D.K. Dutta, Adsorption of Cr(VI) in layered double hydroxides, Appl. Clay Sci. 13 (1998) 21–34.
[9] S.L. Wang, R.J. Hseu, R.R. Chang, P.N. Chiang, J.H. Chen, Y.M. Tzou, Adsorption and thermal desorption of Cr(VI) on Li/Al layered double hydroxide, Colloids Surf. A: Physicochem. Eng. Aspects 277 (2006) 8–14.
[10] E. Demirbas, M. Kobya, A.E.S. Konukman, Error analysis of equilibrium studies for the almond shell activated carbon adsorption of Cr(VI) from aqueous solutions, J. Hazard. Mater. 154 (2008) 787–794.
[11] M. Kobya, Removal of Cr(VI) from aqueous solutions by adsorption onto hazelnut shell activated carbon: kinetic and equilibrium studies, Bioresour. Technol. 91 (2004) 317–321.
[12] X.S. Wang, Y.P. Tang, S.R. Tao, Kinetics, equilibrium and thermodynamic study on removal of Cr (VI) from aqueous solutions using low-cost adsorbent Alligator weed, Chem. Eng. J. 148 (2009) 217–225.
[13] B.S. Krishna, D.S.R. Murty, B.S. Jai Prakash, Surfactant-modified clay as adsorbent for chromate, Appl. Clay Sci. 20 (2001) 65–71.
[14] M. Ghiaci, R. Kia, A. Abbaspur, F. Seyedeyn-Azad, Adsorption of chromate by surfactant-modified zeolites and MCM-41 molecular sieve, Sep. Purif. Technol. 40 (2004) 285–295.
[15] R. Leyva-Ramos, A. Jacobo-Azuara, P.E. Diaz-Flores, R.M. Guerrero-Coronado, J. Mendoza-Barron, M.S. Berber-Mendoza, Adsorption of chromium(VI) from an aqueous solution on a surfactant-modified zeolite, Colloids Surf. A: Physicochem. Eng. Aspects 330 (2008) 35–41.
[16] Y. Huang, X.Y. Ma, G.Z. Liang, Y.X. Yan, S.H. Wang, Adsorption behavior of Cr(VI) on organic-modified rectorite, Chem. Eng. J. 138 (2008) 187–193.
[17] C. Cooper, J.Q. Jiang, S. Ouki, Preliminary evaluation of polymeric Fe- and Al-modified clays as adsorbents for heavy metal removal in water treatment, J. Chem. Technol. Biotechnol. 77 (2002) 546–551.
[18] C.B. Molina, J.A. Casas, J.A. Zazo, J.J. Rodriguez, A comparison of Al–Fe and Zr–Fe pillared clays for catalytic wet peroxide oxidation, Chem. Eng. J. 118 (2006) 29–35.
[19] Y.S. Shin, S.G. Oh, B.H. Ha, Pore structures and acidities of Al-pillared montmorillonite, Kor. J. Chem. Eng. 20 (2003) 77–82.
[20] M.R. Sun Kou, S. Mendioroz, M.I. Guijarro, A thermal study of Zr-pillared montmorillonite, Thermochim. Acta 323 (1998) 145–157.
[21] L.V. Govea, H. Steinfink, Thermal stability and magnetic properties of Fe-polyoxocation intercalated montmorillonite, Chem. Mater. 9 (1997) 849–856.
[22] C. Volzone, Pillaring of different smectite members by chromium species (Cr-PILCs), Micropor. Mesopor. Mater. 49 (2001) 197–202.
[23] T. Mishra, K. Parida, Transition metal oxide pillared clay: synthesis, characterization and catalytic activity of iron–chromium mixed oxide pillared montmorillonite, Appl. Catal. A: Gen. 174 (1998) 91–98.
[24] S. Moreno, R. Sun Kou, R. Molina, G. Poncelet, Al-, Al, Zr-, and Zr-pillared montmorillonites and saponites: preparation, characterization, and catalytic activity in heptane hydroconversion, J. Catal. 182 (1999) 174–185.
[25] D.L. Guerra, C. Airoldi, V.P. Lemos, R.S. Angelica, Adsorptive, thermodynamic and kinetic performances of Al/Ti and Al/Zr-pillared clays from the Brazilian Amazon region for zinc cation removal, J. Hazard. Mater. 155 (2008) 230–242.
[26] S.L. Tian, P.X. Jiang, P. Ning, Y.H. Su, Enhanced adsorption removal of phosphate from water by mixed lanthanum/aluminum pillared montmorillonite, Chem. Eng. J. 151 (2009) 141–148.
[27] N. Bouchenafa-Saïb, K. Khouli, O. Mohammedi, Preparation and characterization of pillared montmorillonite: application in adsorption of cadmium, Desalination 217 (2007) 282–290.
[28] L.J. Michot, O. Barres, E.L. Hegg, T.J. Pinnavaia, Cointercalation of aluminum (Al_{13}) polycations and nonionic surfactants in montmorillonite clay, Langmuir 9 (1993) 1794–1800.
[29] P. Yuan, F. Annabi-Bergaya, Q. Tao, M.D. Fan, Z.W. Liu, J.X. Zhu, H.P. He, T.H. Chen, A combined study by XRD, FTIR, TG and HRTEM on the structure of delaminated Fe-intercalated/pillared clay, J. Colloid Interface Sci. 324 (2008) 142–149.
[30] P.X. Wu, W.M. Wu, S.Z. Li, N. Xing, N.W. Zhu, P. Li, J.H. Wu, C. Yang, Z. Dang, Removal of Cd^{2+} from aqueous solution by adsorption using Fe–montmorillonite, J. Hazard. Mater. 169 (2009) 824–830.
[31] Q.Q. Chen, P.X. Wu, Y.Y. Li, N.W. Zhu, Z. Dang, Heterogeneous photo-Fenton photodegradation of reactive brilliant orange X-GN over iron-pillared montmorillonite under visible irradiation, J. Hazard. Mater. 168 (2009) 901–908.
[32] J.Q. Jiang, N.J.D. Graham, Enhanced coagulation using Al/Fe(III) coagulants: effect of coagulant chemistry on the removal of colour-causing NOM, Environ. Technol. 17 (1996) 937–950.
[33] M.X. Zhu, K.Y. Ding, S.H. Xu, X. Jiang, Adsorption of phosphate on hydroxyaluminum– and hydroxyiron–montmorillonite complexes, J. Hazard. Mater. 165 (2009) 645–651.

[34] A. Gil, A. Massinon, P. Grange, Analysis and comparison of the microporosity in Al-, Zr-, Ti-pillared clays, Micropor. Mater. 4 (1995) 369–378.
[35] I. Heylen, E.F. Vansant, The difference in adsorption capacity between Fe-PILCs and modified Fe-BuA- and Fe–Zr-PILCs, Micropor. Mater. 10 (1997) 41–50.
[36] J. Hu, I.M.C. Lo, G.H. Chen, Fast removal and recovery of Cr(VI) using surface-modified jacobsite ($MnFe_2O_4$) nanoparticles, Langmuir 21 (2005) 11173–11179.
[37] D. Nguyen-Thanh, K. Block, T.J. Bandosz, Adsorption of hydrogen sulfide on montmorillonites modified with iron, Chemosphere 59 (2005) 343–353.
[38] B.G. Mishra, G.R. Rao, Physicochemical and catalytic properties of Zr-pillared montmorillonite with varying pillar density, Micropor. Mesopor. Mater. 70 (2004) 43–50.
[39] J.R. Sohn, J.T. Kim, Infrared study of alkyl ketones adsorbed on the interlamellar surface of montmorillonite, Langmuir 16 (2000) 5430–5434.
[40] J. Madejova, FTIR techniques in clay mineral studies, Vib. Spectrosc. 31 (2003) 1–10.
[41] J. Manjanna, T. Kozaki, S. Sato, Fe(III)–montmorillonite: basic properties and diffusion of tracers relevant to alteration of bentonite in deep geological, Appl. Clay Sci. 43 (2009) 208–217.
[42] P. Yuan, M.D. Fan, D. Yang, H.P. He, D. Liu, A.H. Yuan, J.X. Zhu, T.H. Chen, Montmorillonite-supported magnetite nanoparticles for the removal of hexavalent chromium [Cr(VI)] from aqueous solutions, J. Hazard. Mater. 166 (2009) 821–829.
[43] B.S. Krishna, D.S.R. Murty, B.S. Jai Prakash, Thermodynamics of chromium(VI) anionic species sorption onto surfactant-modified montmorillonite clay, J. Colloid Interface Sci. 229 (2000) 230–236.
[44] A. Ramesh, H. Hasegawa, T. Maki, K. Ueda, Adsorption of inorganic and organic arsenic from aqueous solutions by polymeric Al/Fe modified montmorillonite, Sep. Purif. Technol. 56 (2007) 90–100.
[45] M. Dimitri, G. Vladimir, W. Abraham, Ion Exchange, Marcel Dekker, New York, 2000.
[46] Y.H. Wang, L. Ye, Y.H. Hu, Adsorption mechanisms of Cr(VI) on the modified bauxite tailings, Miner. Eng. 21 (2008) 913–917.
[47] A.K. Bhattacharya, T.K. Naiya, S.N. Mandal, S.K. Das, Adsorption, kinetics and equilibrium studies on removal of Cr(VI) from aqueous solutions using different low-cost adsorbents, Chem. Eng. J. 137 (2008) 529–541.
[48] Q.Z. Li, L.Y. Chai, Z.H. Yang, Q.W. Wang, Kinetics and thermodynamics of Pb(II) adsorption onto modified spent grain from aqueous solutions, Appl. Surf. Sci. 255 (2009) 4298–4303.
[49] Y.C. Sharma, Uma, V. Srivastava, J. Srivastava, M. Mahto, Reclamation of Cr(VI) rich water and wastewater by wollastonite, Chem. Eng. J. 127 (2007) 151–156.